ELSEVIER

Inorganica Chimica Acta 338 (2002) 235–239

Inorganica Chimica Acta

www.elsevier.com/locate/ica

Note

Kinetic studies on thiolato-ligand substitution reactions with halide ions of square-planar palladium(II) complex with bis(2-(diphenylphosphino)ethyl)phenylphosphine

Sen-ichi Aizawa [a,*], Yasushi Sone [b], Tatsuya Kawamoto [c], Shinkichi Yamada [b], Motoshi Nakamura [b]

[a] *Faculty of Engineering, Toyama University, 3190 Gofuku, Toyama 930-8555, Japan*
[b] *Faculty of Engineering, Shizuoka University, Johoku, Hamamatsu 432-8561, Japan*
[c] *Department of Chemistry, Graduate School of Science, Osaka University, 1-16 Machikaneyama, Toyonaka, Osaka 560-0043, Japan*

Received 11 January 2002; accepted 5 April 2002

Abstract

The square-planar thiolato palladium(II) complex with a terdentate phosphine bound ligand, $[Pd(pt)(p_3)](BF_4)$ (p_3 = bis(2-(diphenylphosphino)ethyl)phenylphosphine, pt = 1-propanethiolate) has been synthesized and characterized by ^{31}P NMR spectroscopy. The solid state structure of $[PdI(p_3)]I$ was determined by an X-ray crystal structure analysis. The kinetic parameters for the thiolato-ligand substitution reactions with halide ions, $[Pd(pt)(p_3)]^+ + X^- \rightarrow [PdX(p_3)]^+ + pt^-$ ($X^- = Cl^-$, Br^-, I^-), in chloroform were obtained as follows: $k^{298} = 7.22$, 1.68 and 10.1×10^{-4} s^{-1}, $\Delta H^{\ddagger} = 67 \pm 2$, 56 ± 2 and 63 ± 3 kJ mol^{-1} and $\Delta S^{\ddagger} = -80 \pm 7$, -128 ± 6 and -92 ± 11 J mol^{-1} K^{-1}, respectively. These kinetic results are compared with those for the corresponding reactions of the trigonal-bipyramidal complex with an analogous phosphine bound ligand, $[Pd(pt)(pp_3)](BF_4)$ (pp_3 = tris(2-(diphenylphosphino)ethyl)phosphine).

Keywords: Square-planar palladium(II) complexes; Thiolato complexes; Substitution reaction; Reaction mechanism

1. Introduction

Recently, we have performed the mechanistic studies on five-coordinate trigonal-bipyramidal palladium(II) complexes [1,2] to compare the reaction mechanism with that for four-coordinate square-planar ones which had been extensively studied so far [3]. However, in order to make a precise comparison of the reaction mechanism for both geometries, comparable reaction system including the same entering and leaving ligands, coordinated atoms or groups in the bound ligands, solvent and counter ion should be investigated. Since we previously reported the kinetics for thiolato-ligand substitution reactions with halide ions in chloroform by using trigonal-bipyramidal $[Pd(pt)(pp_3)](BF_4)$ (pp_3 = tris(2-(diphenylphosphino)ethyl)phosphine, pt = 1-propanethiolate) [2], the kinetic studies on the corresponding reactions of the square-planar analog $[Pd(pt)(p_3)](BF_4)$ (p_3 = bis(2-(diphenylphosphino)ethyl)phenylphosphine) have been carried out.

2. Experimental

2.1. Reagents

Chloroform (Wako, ∞ pure) and deuterated chloroform (Wako, 100%) were dried over activated 4A Molecular Sieves. Tetrabuthylammonium halides (Wako), Bu_4NX ($X^- = Cl^-$, Br^-, and I^-), were dried under a vacuum. Bis(2-(diphenylphosphino)ethyl)phenylphosphine (p_3, Strem, 97%) and 1-propanethiol (Hpt, Wako) were used to prepare palladium(II) complexes without further purification.

* Corresponding author. Tel./fax: +81-76-445 6980
E-mail address: saizawa@eng.toyama-u.ac.jp (S.-i. Aizawa).

0020-1693/02/$ - see front matter
PII: S0020-1693(02)00981-7

2.2. Preparation of complexes

2.2.1. [Pd(pt)(p$_3$)](BF$_4$)

To a solution of [Pd(p$_3$)(CH$_3$CN)](BF$_4$)$_2$ [4] (0.32 g, 0.37 mmol) in acetonitrile (30 cm^3) was added dropwise 1-propanethiol (Hpt, 0.045 g, 0.59 mmol), and then ethanol (5 cm^3) and 0.1 M aqueous NaOH (1 cm^3). The resultant yellow solution was filtered, and water (ca. 15 cm^3) was added to the filtrate to give yellow crystals. The crystals were collected by filtration and recrystallized from dichloromethane by adding ethanol and water. Yield: 0.20 g (67%). *Anal.* Calc. for [Pd(p$_3$)(pt)](BF$_4$): C, 55.35; H, 5.02; N, 0.00. Found: C, 55.62; H, 4.98; N, 0.00%. ^{31}P NMR (in CHCl$_3$): δ (relative to D$_3$PO$_4$ in external D$_2$O) = 48.93 (d, terminal), 101.59 (t, central); J_{P-P} = 20.8 Hz.

2.2.2. [PdX(p$_3$)]X ($X^- = Cl^-$, Br^-, I^-)

The halo complexes were prepared by the procedures described previously [1]. Single crystals of the iodo complex were obtained by slow evaporation of the dichloromethane solution containing a small amount of ethanol and water. ^{31}P NMR (in CHCl$_3$) for the chloro, bromo and iodo complexes: δ (relative to D$_3$PO$_4$ in external D$_2$O) = 45.87, 46.78 and 47.20 (d, terminal), 111.20, 112.77 and 111.62 (t, central); J_{P-P} = 10.0, 8.3 and 7.3 Hz, respectively.

2.3. X-ray structure analysis

X-ray diffraction measurements for the iodo complex were performed on a Mac Science MXC3 diffractometer with Mo Kα radiation. The unit-cell parameters and orientation matrix were determined by a least-squares refinement of 22 independent reflections collected in the range of $3.0^\circ < 2\theta < 35.0^\circ$. Data collection was performed with the θ–2θ scan mode with three standard reflections measured after every 100 scans, which showed no significant decay. An empirical absorption (ψ scan) correction was applied. The solution and refinement were carried out using CRYSTAN-GM (version 6.3.3) [5]. The structure was solved by direct methods using the programs of SIR 92 [6]. All non-hydrogen atoms were refined anisotropically and hydrogen atoms were included in the calculated positions (C–H = 0.96 Å). The atomic scattering factors were taken from ref. [7]. With Z = 8, the complex cation and counter ion sit on the crystallographic mirror plane 1/2, y, z; 15 atoms have such coordinates (Pd(1), I(1), I(2), P(2), C(15)–C(20) and H(16)–H(20)).

The crystallographic data are summarized in Table 1. The crystallographic details, positional and thermal parameters for all atoms, and bond distances and angles for non-hydrogen atoms are provided as Section 4.

Table 1
Crystallographic data for [PdI(p$_3$)]I

Empirical formula	$C_{34}H_{33}I_2P_3Pd$
Formula weight	894.79
Temperature (K)	298
Crystal habit	polyhedron
Crystal size (mm)	0.20 × 0.20 × 0.20
Crystal system	tetragonal
Space group	$I4_1md$
a (Å)	24.23(1)
c (Å)	12.430(3)
V (Å^3)	7298(5)
Z	8
D_{calc} (g cm^{-3})	1.629
μ (cm^{-1})	2.326
R [a], R_w [b]	0.118, 0.140

[a] $R = \Sigma||F_o| - |F_c||/\Sigma|F_o|$.
[b] $R_w = [\Sigma\ w(|F_o| - |F_c|)^2/\Sigma\ w|F_o|^2]^{1/2}$. $w = (\sigma^2(F_o) + 0.001F_o^2)^{-1}$.

2.4. Measurements

The kinetic measurements for the substitution reactions of the pt complex with halide ions in chloroform were carried out under pseudo-first-order conditions where the concentrations of Bu$_4$NX ($X^- = Cl^-$, Br^-, I^-) were in large excess over those of the complex (Tables S5 and S6, Section 4). The sample preparation and kinetic measurements were performed under a nitrogen atmosphere. The absorption spectral changes were recorded on a JASCO V-570 spectrophotometer. The temperature of the reaction solution was controlled within ±0.1 K. The ^{31}P NMR spectra were recorded on a JEOL JNM-A400 FT-NMR spectrometer operating at 160.7 MHz. In order to determine the chemical shift of the ^{31}P NMR, a 3 mm o.d. NMR tube containing the sample solution was coaxially mounted in a 5 mm o.d. NMR tube containing deuterated water and phosphoric acid as a lock solvent and a reference, respectively.

3. Results and discussion

3.1. Characterization

A perspective view of the iodo complex cation is displayed in Fig. 1 along with the atomic labeling. The complex cation has a square-planar geometry with a mirror plane bisecting the p$_3$ ligand. The coordination bond distance for the central phosphine (P(2)) is considerably shorter than those for the terminal ones (P(1)), probably due to the weak trans influence of the iodo ligand compared with that of the diphenylphosphino group and the chelate strain of the two five-membered chelate rings in the terdentate p$_3$ ligand (P(1)–Pd(1)–P(2) = 84.3° and P(1)–Pd(1)–I(1) = 96.1°). In Table 2, the coordination bond distances of the iodo complex are compared with those of the

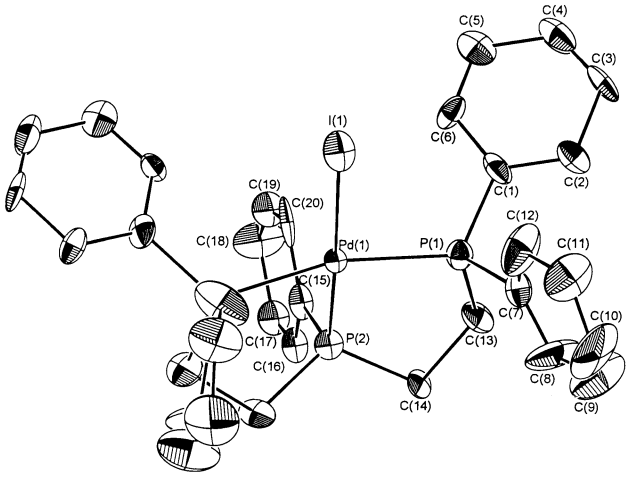

Fig. 1. ORTEP diagram of $[PdI(p_3)]^+$.

Table 2
Coordination bond distances (Å) of $[PdI(p_3)]^+$, $[Pd(CF_3SO_3)(p_3)]^+$ and $[PdI(pp_3)]^+$

$[PdI(p_3)]^+$	
Pd(1)–I(1)	2.672(10)
Pd(1)–P(1)	2.311(14)
Pd(1)–P(2)	2.24(3)
$[Pd(CF_3SO_3)(p_3)]^+$	
Pd–O	2.127(7)
Pd–P_t [a]	2.344 [e]
Pd–P_c [b]	2.192(2)
$[PdI(pp_3)]^+$	
Pd–I	2.687 [e]
Pd–P_{eq} [c]	2.42 [e]
Pd–P_{ax} [d]	2.23 [e]

[a] Terminal phosphorus.
[b] Central phosphorus.
[c] Equatorial phosphorus.
[d] Axial phosphorus.
[e] Average value.

corresponding square-planar trifluoromethanesulfonato complex, $[Pd(CF_3SO_3)(p_3)]^+$ [8] and the trigonal-bipyramidal iodo complex with a tripodal tetradentate phosphine ligand, $[PdI(pp_3)]^+$ [1]. The bond distance for the central phosphorus atom of $[PdI(p_3)]^+$ is a little longer than that for $[Pd(CF_3SO_3)(p_3)]^+$. This suggests that the trans influence of the iodo ligand is stronger than that of the sulfonato oxygen. The bond distance for the terminal phosphorus atom of $[PdI(p_3)]^+$ is considerably shorter than the average bond distance for those of $[PdI(pp_3)]^+$. This is due to strong σ interactions in the square plane for the former compared with those in the equatorial plane for the latter although it is possible that π interactions are stronger in the latter case. On the other hand, the axial coordination bond distances for the central phosphorus atom and iodo ligand in the trigonal-bipyramidal geometry are comparable to the corresponding bond distances in the square-planar geometry in spite of the larger ionic radius of the five-coordinate ion. This fact indicates the relatively strong σ interactions of the axial coordination bonds for the trigonal-bipyramidal geometry.

The pt and halo complexes exhibit two ^{31}P NMR signals (triplet and doublet) corresponding to the central and equivalent terminal phosphorus atoms, respectively (see Section 2). Such a spectral pattern is consistent with the square-planar geometry with C_{2v} symmetry. In the case of the free p_3 ligand, the ^{31}P NMR signal of the central phosphorus atom shows an upfield shift compared with that of the terminal phosphorus atoms in the diphenylphosphino groups [9]. However, the downfield shift for the central phosphorus atom is much larger than that of the terminal phosphorus atoms in the present complexes. This is explained by the greater deshielding (diamagnetic contribution) and configurational ununiformity of the valence electrons (paramagnetic contribution) on the phosphorus atoms caused by the stronger donation of the central phosphorus atom, which is observed in the Pd–P bond distances [10,11]. The upfield shift for the central phosphorus atom of the pt complex compared with the halo complexes is attributed to the stronger trans influence of the thiolato sulfur atom.

3.2. Kinetics

The ^{31}P NMR spectra of solutions containing the pt complex and a large excess of Bu_4NX ($X^- = Cl^-$, Br^-, I^-) in chloroform gradually changed to those of the corresponding halo complexes. The absorption spectra of the diluted solutions (4.15×10^{-5}–4.66×10^{-5} mol kg^{-1} of the pt complex and 2.60×10^{-2}–4.58×10^{-1} mol kg^{-1} of Bu_4NX in chloroform) changed with isosbestic points and finally exhibited the spectra of the corresponding halo complexes (Fig. S1). The observed pseudo-first-order rate constants of the pt ligand substitution reactions with halide ions (k) were determined by a nonlinear least-squares analysis for the exponential time course of the absorbance (Fig. S1).

The values of k were independent of the halide-ion concentration (Table S5). Since the limiting dissociative mechanism is not consistent with the fact that the present kinetic parameters depend on the entering halide ions and the values of $\Delta S^{\ddagger}$ are considerably negative (vide infra), it is probable that ion pairs of the positively charged pt complex with halide ions existing in large excess are quantitatively formed in chloroform as usually observed in weakly-polar solvents [12]. Such a ion-pair mechanism was also observed in the case of the corresponding reactions of the trigonal-bipyramidal pt complex, $[Pd(pt)(pp_3)]^+$ [2], and was closely reported for the ligand substitution reactions of the square-planar platinum(II) complex [13]. Each temperature dependence of the first-order rate constant was fitted to the

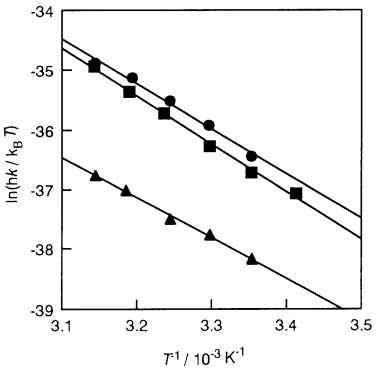

Fig. 2. Temperature dependence of the rate constants for the thiolato-ligand substitution reactions with Cl^- (■), Br^- (▲) and I^- (●).

Eyring equation as shown in Fig. 2 to give the values of $\Delta H^{\ddagger}$ and $\Delta S^{\ddagger}$ (Table S6). The activation parameters obtained are summarized in Table 3 together with those for the corresponding reactions of the trigonal-bipyramidal pt complex.

It is apparent that the mode of activation for the square-planar pt complex becomes more associative than that for the trigonal-bipyramidal one showing the smaller positive values of $\Delta H^{\ddagger}$ and larger negative values of $\Delta S^{\ddagger}$ (Table 3). The difference in the reaction mechanism is explained by the difference in the electronic repulsion in the transition state, because, the four-coordinate square-planar ground state with the 16-electron system can easily accept the coming-ligand orbital compared with the five-coordinate trigonal-bipyramidal one with the 18-electron system.

Another point worth mentioning is the mechanistic change caused by the difference in the coming halide ions. In the case of the trigonal-bipyramidal complex, the enhancement of the dissociative character from Cl^- to I^- is ascribed to an increase in the steric hindrance of the crowded substitution site. On the other hand, even considering the electron-accepting ability, $I^- > Br^- > Cl^-$, we can not explain by the steric or electronic factor why the activation mode of the square-planar complex is the most associative in the case of the reaction with Br^-.

Table 3
Activation parameters for substitution reactions of $[Pd(p_3$ or pp_3 [a]$)(pt)]^+$ with halide ions

Bound ligand	Halide ion	k^{298} (10^{-4} s^{-1})	$\Delta H^{\ddagger}$ (kJ mol^{-1})	$\Delta S^{\ddagger}$ (J mol^{-1} K^{-1})
p_3	Cl^-	7.22	67±2	−80±7
p_3	Br^-	1.68	56±2	−128±6
p_3	I^-	10.1	63±3	−92±11
pp_3	Cl^-	3.55	70±2	−77±5
pp_3	Br^-	2.76	82±2	−37±7
pp_3	I^-	2.14	89±1	−16±2

[a] Ref. [2].

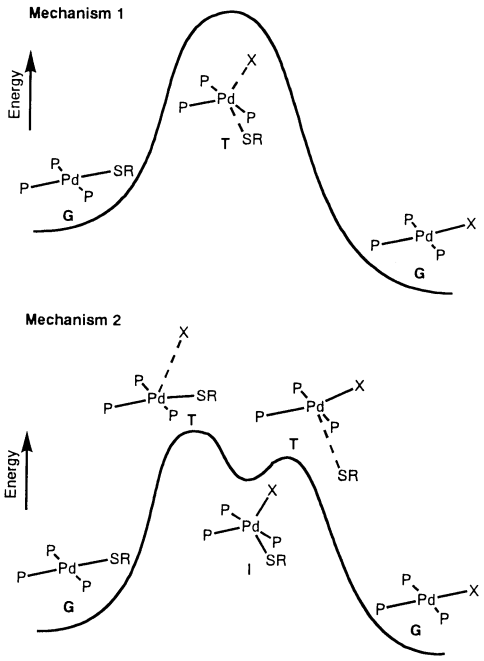

Fig. 3. Two reaction mechanisms for the square-planar palladium(II) complexes. G, T and I denote the ground state, transition state and intermediate, respectively.

So far, an associative mechanism via a trigonal-bipyramidal transition state or intermediate has been proposed for substitution reactions of square-planar palladium(II) and platinum(II) complexes (Fig. 3) [3,14]. If the intermediate is formed, the observed activation parameters correspond to the energy level of the preceding transition state in which the coming ligand is less bound than in the intermediate (Mechanism 2 in Fig. 3). Furthermore, the transition state in Mechanism 2 (Fig. 3) can be more dissociative compared with the trigonal-bipyramidal transition state in Mechanism 1 (Fig. 3). Considering that the intermediate is likely to be formed in systems with π-accepting ligands such as phosphine and I^- [15,16], the deviation in the order of the activation parameters for $[Pd(pt)(p_3)]^+$ may be attributed to the formation of the intermediate in the case of the reaction with I^-.

4. Supplementary material

An X-ray crystallographic data (Table S1), atomic coordinates and isotropic thermal parameters (Table S2), anisotropic thermal parameters (Table S3), bond distances and angles (Table S4), entering-ligand concentration (Table S5) and temperature (Table S6) dependences of rate constants, absorption spectral changes for substitution reactions (Fig. S1) (in total nine pages) are available from the author upon request.

Acknowledgements

This research was supported by Grant-in-Aid for Scientific Research (No. 12640583) from the Ministry of Education, Culture, Sports, Science and Technology of Japan.

References

[1] S. Aizawa, T. Iida, S. Funahashi, Inorg. Chem. 35 (1996) 5163.
[2] S. Aizawa, T. Iida, Y. Sone, T. Kawamoto, S. Funahashi, S. Yamada, M. Nakamura, Bull. Chem. Soc. Jpn. 75 (2002) 91.
[3] (a) R.G. Wilkins, Kinetics and Mechanism of Reaction of Transition Metal Complexes, second ed. (Chapter 4), VCH, Weinheim, 1991;
(b) R.J. Cross, M.V. Twigg, Mechanisms of Inorganic and Organometallic Reactions, (Chapter 5), Plenum, New York, 1988.
[4] D.L. DuBois, A. Miedaner, J. Am. Chem. Soc. 109 (1987) 133.
[5] Programs for X-ray Crystal Structure Determination, MAC Science, Yokohama, 1994.
[6] A. Altomare, G. Cascarano, C. Giacovazzo, A. Guagliardi, J. Appl. Crystallogr. 26 (1993) 343.
[7] International Tables for X-ray Crystallography, vol. IV, Kynoch, Birmingham, AL, 1974.
[8] S. Aizawa, T. Yagyu, K. Kato, S. Funahashi, Anal. Sci. (1995) 557.
[9] ^{31}P NMR (in $CHCl_3$): δ (relative to D_3PO_4 in D_2O) = −16.71 (t, central), −13.00 (d, terminal); $J_{P-P} = 28.9$ Hz.
[10] C.J. Jameson, H.S. Gutowsky, J. Chem. Phys. 40 (1964) 1714.
[11] N.F. Ramsey, Phys. Rev. 77 (1950) 567.
[12] L. Song, W.C. Trogler, J. Am. Chem. Soc. 114 (1992) 3355.
[13] G. Alibrandi, R. Romeo, L.M. Scolaro, M.L. Tobe, Inorg. Chem. 31 (1992) 5061.
[14] Z. Lin, M.B. Hall, Inorg. Chem. 30 (1991) 646.
[15] F.A. Cotton, G. Wilkinson, Advanced Inorganic Chemistry, Wiley, New York, 1988, pp. 1299–1300.
[16] R.B. Jordan, Reaction Mechanisms of Inorganic and Organometallic Systems, Oxford University Press, Oxford, 1991, p. 58.